DEVELOPMENTS IN
EARTH SURFACE PROCESSES

7

ELSEVIER

CATCHMENT DYNAMICS AND RIVER PROCESSES

MEDITERRANEAN AND OTHER CLIMATE REGIONS

EDITED BY

C. GARCIA AND R.J. BATALLA

7
GARCIA
BATALLA
EDITORS
CATCHMENT DYNAMICS AND RIVER PROCESSES
MEDITERRANEAN AND OTHER CLIMATE REGIONS

Catchment Dynamics and River Processes: Mediterranean and Other Climate Regions
Celso Garcia, Ramon J. Batalla, Editors

Chapter 10

Maintenance of an obstruction-forced pool in a gravel-bed channel: streamflow, channel morphology, and sediment transport

Richard D. Woodsmith[1,*] and Marwan A. Hassan[2]

[1]*USDA, Forest Service, Pacific Northwest Research Station, 1133 N, Western Ave., Wenatchee, WA 98801, USA*

[2]*Department of Geography, University of British Columbia, Vancouver, B.C. V6T 1Z2, Canada*

Abstract

Maintenance of pool morphology in a stream channel with a mobile bed requires hydraulic conditions at moderate to high flows that route bed load through the pool as it is delivered from upstream. Through field measurements of discharge, vertical velocity profiles, bed load transport, and streambed scour, fill, and grain-size distribution, we found that maintenance of a pool associated with a large, in-channel obstruction was more adequately explained by analogy to scour processes at bridge abutments than by the concept of velocity reversal. The cross-sectional area through the deepest part of the pool remained remarkably stable throughout a wide range in discharge magnitude. This occurred despite transport of significant quantities of bed load from upstream through the pool, well above and well below bankfull discharge and on rising as well as falling hydrograph limbs. There was no tendency for near-bed velocity or shear stress (averaged over the cross-sectional width of active bed load transport) at the pool centre to exceed that at the upstream riffle tail (pool head) or downstream riffle head (pool tail) as discharge increased up to at least 1.3 times bankfull. Fractional rates indicated that at the pool centre significant bed load transport was initiated and approached 100 g m^{-1} s^{-1} at notably lower mean bed shear stress than at the pool head or tail. Furthermore, incipient motion analyses suggested that mean bed shear stress entrainment thresholds were lower at the pool centre than at the pool head or tail. These findings indicated that total entrainment force in the pool was underestimated by average bed shear stress alone. Through inference, rather than direct measurement, we concluded that, as at bridge abutments, turbulent effects generated by interaction of streamflow with the obstruction added a component of total entrainment force. We further inferred that this combination of mean bed shear stress and instantaneous turbulent force was responsible for entrainment and transport of sediment, thereby maintaining pool morphology. This conceptual model of pool maintenance through a combination of mean bed shear stress and large-scale turbulent force suggests that flow obstructions in gravel-bed streams may be a dominant factor, perhaps as important as mean hydraulic variables or caliber and volume of sediment supply, in controlling local channel morphology and local bed load dynamics.

Keywords: pool-riffle, scour and fill, bed load, flow obstructions, mountain streams

1. Introduction

Pool-riffle sequences are a fundamental morphologic expression of interactive adjustments among hydraulics, bed scour, and sediment transport and deposition in lower- to moderate-gradient streams. They are also responsible for generating a diverse range of hydraulic and biological niches, which are critical in sustaining high-quality river habitats. Pools can be loosely defined as topographic depressions in the channel bed (Montgomery and Buffington, 1997). Although a minimum size is necessarily implied or stated explicitly (Woodsmith and Buffington, 1996), there is no general agreement on a precise definition.

Understanding formation and maintenance of pools is problematic, because at low discharge pools are relatively low energy environments, characterized by slower, convergent flow, lower water surface slopes, and finer bed surface material than are riffles. Nevertheless, during high discharge events when bed load is being transported, if stream competence is not at least as large in pools as it is immediately upstream, then sediment continuity will not be maintained and pools will aggrade. Pools commonly persist despite a mobile bed and annual bed load yields far larger than pool volume. In gravel-bed streams in valley bottoms, pool formation and maintenance has been attributed to scour along a series of alternate bars by converging flow opposite the slip face of each bar, whereas riffles form on the stoss side of these bars. Downstream of the pool, flow diverges, shear stress is reduced, and bed load is deposited at another bar (Richards, 1976; Church and Jones, 1982). Understanding the controls on streambed topography and pool maintenance in free-formed, alluvial channels has also been approached through detailed modeling of the interactive adjustments of velocity, boundary shear stress, and gravitational and centrifugal forces influencing sediment transport and water surface and bed topography (Dietrich et al., 1979; Nelson and Smith, 1989).

Perhaps the best known model of pool-riffle maintenance is provided by the "velocity (or shear stress) reversal hypothesis," which describes a reversal in the location of maximum near-bed velocity or shear stress from riffles to pools as discharge increases to about bankfull. According to this hypothesis, as discharge increases during high flow events, energy slope, near-bed velocity, and shear stress increase more rapidly at pools than at riffles until, at about bankfull discharge, the magnitude of these entrainment parameters becomes greater in pools than in riffles (Leopold and Wolman, 1960; Keller, 1971; Richards, 1976; Lisle, 1979). This reversal causes sediment to be transported through the pool and, provided sufficiently low transport energy, deposited on a downstream riffle. Thus, pools are believed to fill during falling hydrograph limbs and low flow and to scour during rising discharge and high flow, whereas riffles do the reverse, thereby maintaining pool-riffle morphology (Andrews, 1979; Parker and Peterson, 1980; Ashworth, 1987).

The studies cited above as well as several others tend to support aspects of the velocity reversal concept (e.g., Emmett et al., 1983; Dietrich and Whiting, 1989; Carling and Wood, 1994; Robert, 1997). Cao et al. (2003) find that flow reversal can occur in specific circumstances in association with a channel constriction. Similarly, Wilkinson et al. (2004) attribute maintenance of pool-riffle sequences to channel-width related phase shifts in location of shear stress maxima and minima as discharge changes.

Considerable uncertainties remain surrounding general acceptance of the velocity reversal hypothesis. In part, these originate with different approaches to the problem. Many studies rely on spatially averaged values of velocity and shear stress rather than local values, which directly affect bed load transport. An additional concern is use of the depth–slope product to calculate shear stress. This method assumes steady, uniform flow and may therefore provide misleading results for unsteady, nonuniform flows in pool-riffle sequences (Paola and Mohrig, 1996; Buffington and Montgomery, 1999a). Clifford and Richards (1992) point out that the velocity reversal hypothesis relies on three major assumptions: (1) that hydraulic power laws hold over the entire range of discharge; (2) these relations are similar for riffles and pools in straight and meandering channels; and (3) reversal occurs for all paired cross-sections designated as riffle and pool within a single pool-riffle unit.

Using computer simulations, Carling and Wood (1994) demonstrated that hydraulic behavior varies nonlinearly among pool-riffle pairs as hydraulic roughness, riffle spacing, and pool-to-riffle width ratio vary. This can produce important effects on spatial variation in competence and on the discharge at which a shear stress reversal may occur. In a review of recent studies, Sear (1996) concluded that not all pool-riffle sequences experience flow reversal, in part because of low competence at pool tails. Furthermore, patterns of scour and fill can be largely explained by differences between pools and riffles in bed surface particle structure. Booker et al. (2001) found that generalized descriptions of hydraulic patterns, such as velocity reversal, were overly simplistic, and routing of sediment by secondary circulation and near-bed flow can strongly influence pool-riffle maintenance. Clearly, additional detailed studies will be necessary to fully understand formation and maintenance of channel morphology in pool-riffle sequences, particularly in more complex channels (Clifford and Richards, 1992; Keller and Florsheim, 1993).

Most of our knowledge surrounding the velocity reversal concept as a general account of pool-riffle maintenance is based on studies conducted in free-formed pools in valley bottom streams, which are generally characterized by relatively low bed load transport rates and unobstructed flow. However, the velocity reversal concept may not be applicable to upland streams with relatively high bed load rates and large, in-channel obstructions such as large boulders or trees transported from upslope or the adjacent riparian zone. In such channels large increases in upstream sediment supply can alter pool-riffle morphology and may even bury these features (Lisle, 1982). Furthermore, processes responsible for maintenance of pools associated with in-channel flow obstructions may differ from processes controlling free-formed pools, in part because of additional large-scale turbulence associated with interaction of flow with the obstruction (Lisle, 1986).

In upland, alluvial streams, pool location is commonly forced by large, in-channel obstructions, and pool morphology can depend strongly on obstruction characteristics (Lisle, 1986; Smith et al., 1993; Hogan et al., 1998; Buffington et al., 2002). Association of pools with in-channel obstructions has been well described (Keller and Swanson, 1979; Lisle, 1986; Montgomery et al., 1995; Buffington et al., 2002). However, only a limited number of studies have directly investigated processes that maintain these pools.

In a flume study simulating bed scour around in-channel logs, Beschta (1983) reported that obstruction analogs created zones of exceptionally high turbulence capable of scouring and transporting gravel, even though mean, near-bed velocities indicated otherwise. This observation suggested that entrainment with rising discharge may be caused by a local increase in obstruction-related turbulence rather than increased average bed shear stress. Thompson et al. (1996, 1999) investigated the effects of a channel constriction and associated recirculating eddy on local competence reversal in a gravel-bed, alluvial stream and in a laboratory analog. At high flow in both settings, the constriction caused convergent, accelerating flow at the head of the pool and a recirculating eddy immediately downstream of the constriction. At the head of the pool and near the constriction, local water surface gradients were higher than at the riffle. In the flume, maximum velocities in the centre of the pool always exceeded maximum velocities at the riffle. However, mean pool velocities were lower because of larger cross-sectional flow area. Thus, pool scour was caused by a local competence reversal in only a portion of the pool.

1.1. Conceptual model of pool maintenance

The purpose of this chapter is to present data from field measurements of discharge, vertical velocity distribution, bed load transport, and streambed scour, fill, and grain-size distribution from a case study in support of a conceptual model explaining maintenance of obstruction-forced pools in gravel-bed streams with high sediment transport rates. Specifically, we are concerned with flow and sediment transport regimes that maintain channel morphology over a wide range of flow conditions, including very high discharge.

Results of a large number of studies analyzing scour at bridge abutments and piers are available in the literature; these are summarized in Breusers et al. (1977); Melville (1997). In the current chapter we draw upon findings and insights from this previous research to support a conceptual model of analogous scouring processes at naturally occurring, in-channel obstructions. We propose this obstruction-forced scour model as an alternative to the velocity reversal concept to explain maintenance of many pools in upland streams. In an earlier chapter we presented relations among channel dynamics, sediment entrainment, and bed load transport and grain size distribution at the same site (Hassan and Woodsmith, 2004).

According to this obstruction-forced scour model, pool scour adjacent to large, in-channel obstructions, such as large boulders or trees, closely resembles scour at bridge piers and abutments (Lisle, 1986; Smith, 1990; Buffington et al., 2002). Accordingly, pool morphology is maintained by scour and sediment transport driven by a combination of mean local bed shear stress and instantaneous lift and drag forces associated with large-scale turbulence generated by interactions of flow with the obstruction.

1.2. Scour processes at bridge abutments and piers

In laboratory studies, and by analogy in the case study presented herein, downward flow at the upstream face of an obstruction induces vortices at the obstruction-bed interface

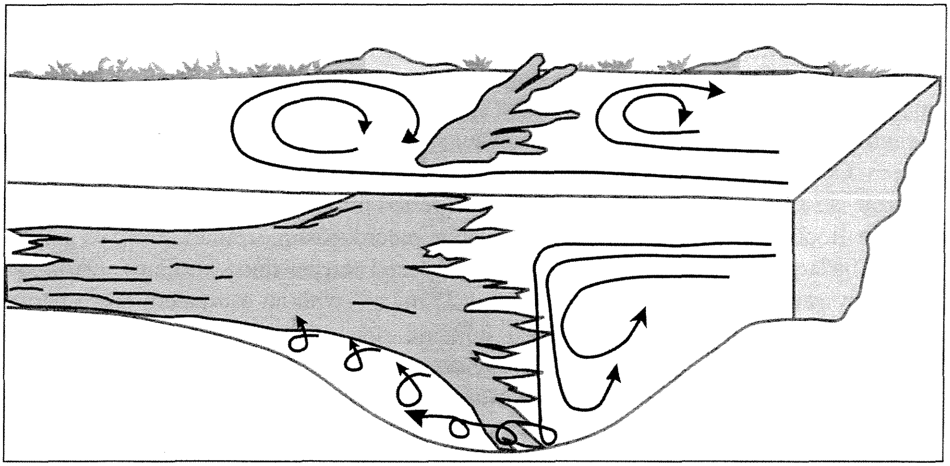

Figure 10.1. Generalized flow patterns and obstruction-related turbulence in a setting similar to the study site.

(Tison, 1961). Vortices with low-pressure centers are cast off near the base of the obstruction, lifting mobile sediment from the bed. Thus, large-scale horseshoe vortices and wake vortices are the primary mechanisms of local scour (Breusers et al., 1977) (Fig. 10.1). Bed material is mobilized by a combination of mean bed shear stress and turbulent agitation both upstream of the obstruction and in the lower portion of the scour hole (Melville, 1975). This combination of hydraulic forces scours pools at an average shear stress less than that required in the absence of obstruction-related scour. Scour may begin at velocities as low as 42% of the critical average velocity for material transport in the unobstructed part of the stream (Tison, 1961; Carstens, 1966; Breusers et al., 1977). Initially size and velocity of near-bed vortices increase rapidly as the new scour hole enlarges, then magnitude of the combined mean bed shear stress and turbulent force at the bed decreases with continued scour until an equilibrium form is reached (Melville, 1975).

Scour depth around engineered structures in gravel-bed channels is greatest at the unobstructed entrainment threshold, and then starts to decrease with stage as upstream sediment is mobilized and delivered to the scour hole. Above this transport threshold, depth undergoes cycles of scour and fill in response to sediment delivery from upstream (Chabert and Engeldinger, 1956; Breusers et al., 1977; Melville, 1984). As flow continues to increase, depth of scour may increase again if scouring in the pool exceeds the rate of sediment input (Melville, 1984; Melville and Sutherland, 1988). Following the discharge peak, pool depth stabilizes when upstream shear stress decreases to the point that bed load is no longer delivered to the pool. This model implies that deeper pools will occur in less mobile alluvial bed material that stabilizes at higher shear stress (Buffington et al., 2002).

2. Study area

Tom McDonald Creek, a tributary to Redwood Creek in north-coastal California, USA, drains an 18-km^2 catchment upslope of the study site, underlain by schist. The climate is Mediterranean with an estimated mean annual precipitation of 203 cm falling primarily between October and April. Floods from rainstorms dominate streamflows. Bankfull discharge is 3.6 m^3 s^{-1}. Gauging records for the period prior to our study are not available; therefore flood frequency was estimated using records from similar, nearby, gauged creeks. The largest peak flow for the study period based on post-flood trimlines and on-site and nearby gauging records was estimated at 25 m^3 s^{-1} with an estimated return period of 5 years (Smith, 1990).

Channel width averaged 10 m at the study site, and the gradient through the reach was 0.006 (Fig. 10.2). Median diameter (D_{50}) of surface material at the pool head, centre, and tail was 31, 3.8, and 17.5 mm, respectively. Median size of subsurface samples (10–40 cm below the bed surface), taken at a riffle immediately downstream of the study pool prior to the largest flood of the study period, was 16 mm. Influence of a large, in-channel obstruction adjacent to the deepest part of the pool (Fig. 10.2) on flow dynamics and channel morphology was obvious from observation. Effective width of this obstruction, perpendicular to flow was 3.6 m, roughly one-third of the active channel width.

The obstruction was a piece of large woody debris (LWD) from the forested catchment. Distribution of LWD in stream channels, its characteristics, and effects on channel morphology and sediment storage and transport have been studied in many places in

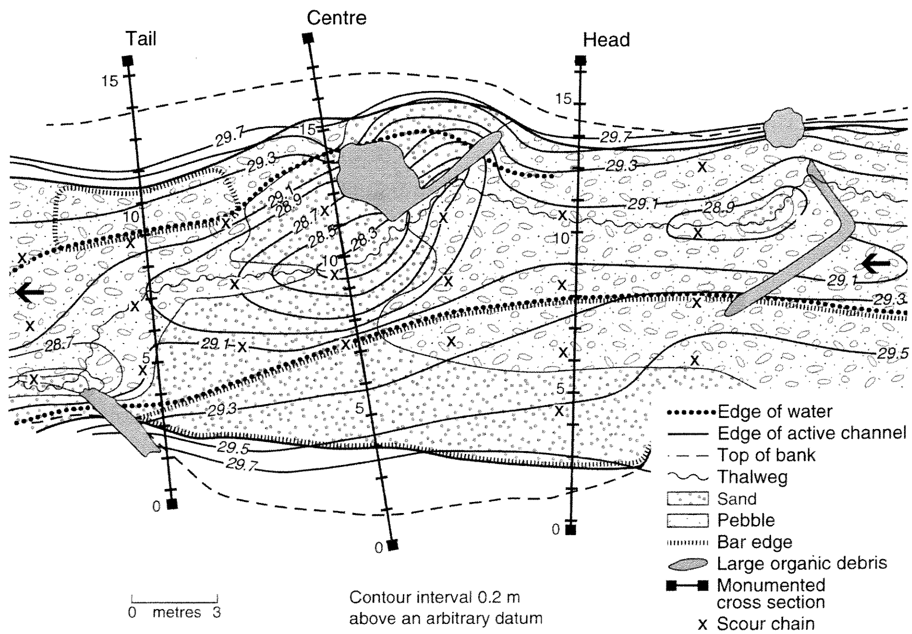

Figure 10.2. Topographic map of the Tom McDonald Creek study site.

the world, including the Pacific coastal region of North America, Mediterranean countries, the United Kingdom, Japan, and others (Keller and Swanson, 1979; Gurnell et al., 1995; Piegay and Gurnell, 1997; Woodsmith and Swanson, 1997). As noted by Piegay and Gurnell (1997), LWD-related effects on flow hydraulics and sediment dynamics commonly affect channel morphology, including pool size and distribution and channel stability.

3. Data collection and analysis

Measurements of flow velocity and direction, bed elevation, and bed load transport were made from three foot bridges following transects perpendicular to the thalweg. Transect 1 was located over the pool head (tail of the upstream riffle); transect 2 over the deepest part of the pool (pool centre), 7 m downstream of the pool head transect; and transect 3 was over the tail of the pool (head of the downstream riffle), 6 m downstream of the pool centre transect (Fig. 10.2). A water level recorder was installed 25 m downstream of the study pool and calibrated against discharge from cross-sectional measurements of velocity, width, and depth. One-minute average velocity and direction of streamflow were measured along vertical profiles spaced at 30 cm or larger intervals across the channel along each transect. Vertical measurement intervals were commonly 2.5 cm at the pool head and pool tail and 15 cm at the pool centre irrespective of flow depth, but larger spacing was sometimes required to complete profiles quickly in rapidly changing flow conditions. In addition to the vertical velocity profiles, several measurements of only the near-bed velocity were made at 30 cm or larger intervals along each transect. Velocity was measured using a standard Price current meter, thus measurements to within 5 cm of the bed were possible. Measurements closer to the bed using other instruments were attempted, but found to be unreliable, owing to interference from bed load and organic material in transport close to the bed. In order to investigate changes in discharge and shear stress relevant to bed load transport, measurements of near-bed velocity, from which shear stress was calculated, were averaged over 2.5 m of channel width, spanning the zone of shear stress maximum and bed load transport.

Local bed shear stress may be derived from a measured velocity gradient using a form of the "law of the wall" equation:

$$\tau_b = \rho \left[(u_2 - u_1) \frac{K}{\ln\left(\frac{z_2}{z_1}\right)} \right]^2 \tag{1}$$

where τ_b is the boundary shear stress at a point, ρ is the density of the fluid, u_2 and u_1 are the point mean velocities at distances z_2 and z_1 measured from and normal to the boundary, and K is the von Karman constant, usually taken to be 0.4 (Middleton and Southard, 1984). We found application of this equation to vertical velocity profiles to be problematic, owing to ambiguity in determining profile slope. Furthermore, shear stress calculated from velocity profiles incorporates shear stress attributable to form drag as well as that attributable to roughness of the bed surface (Dietrich and Whiting, 1989; Buffington and

Montgomery, 1999b). Similarly, shear stress estimates based on the depth–slope product were not used, owing to the difficulty of obtaining an accurate measurement of water surface slope given very complex flow patterns (Carling, 1983; Adams et al., 2000). Eq. 1 can be written as:

$$\tau_b = \rho(u_Z K)^2 \left[\ln\left(\frac{z}{z_0} \right) \right]^{-2} \tag{2}$$

where u_z is the velocity at height z above the bed, z_0, the roughness length, is a constant for fully rough flows equal to approximately $k_s/30$. k_s, the effective roughness height, can be approximated by 3.5 D_x, where D_x is a representative length scale of grains controlling resistance (Hey, 1979; Prestegaard, 1983). Estimating z_0 as 0.1 D_x, the equation further reduces to (Dietrich and Whiting, 1989; Whiting and Dietrich, 1990):

$$\tau_b = \rho(u_Z K)^2 \left[\ln\left(\frac{10z}{D_x} \right) \right]^{-2} \tag{3}$$

We calculated bed shear stress using Eq. 3. Near-bed velocity was estimated using the regression relationship of measured near-bed velocity against dimensionless discharge. z_0 was approximated as 0.1 $D_{50\text{-bedload}}$. We found that the common approach of using bed surface grain size as a measure of roughness length produced unrealistically large values of bed shear stress, comparable to total shear stress computed from the average depth–slope product (see Robert, 1997). Furthermore, our estimates of bed shear stress based on estimating z_0 as 0.1 $D_{50\text{-bedload}}$ agreed closely, over a wide range in discharge, with shear stress back calculated from our measured bed load transport rates, using the Meyer-Peter and Muller (1948) bed load equation. Regression coefficients for relationships of near-bed velocity and shear stress against dimensionless discharge were compared among the three transects employing an analysis of covariance approach (Snedecor and Cochran, 1980) and critical probability level of 0.05.

Direct, near-bed measurement of turbulence is problematic in a high-energy, gravel-bed stream with a mobile bed, owing to changing bed elevation and potential damage to instrumentation (Whiting and Dietrich, 1990; Bunte, 1996). Therefore, we did not attempt such measurements; however, we observed strong turbulent structures, which were obviously related to the obstruction at moderate and greater discharge. These included eddies upstream and downstream of the obstruction and vortices, boils, and upwelling near its edge.

Timing and magnitude of scour and fill were computed from 38 repeat sounding surveys along each of the three transects throughout the study period. These data were supplemented by an array of scour chains (Leopold et al., 1964) used to measure net change in bed elevation (Fig. 10.2). Scour chain data indicated maximum scour, net deposition, and, to some extent, the sequence of scour and fill events. However, a portion of the sediment deposited prior to scouring can be eroded, altering the record of its original thickness.

Bed load transport rates were measured at the three transects using a hand-held, 76 mm-orifice, Helley–Smith bed load sampler (Helley and Smith, 1971) fitted with an enlarged bag to better maintain sampling efficiency (Beschta, 1981). Measurements spanned a wide range in flow from the beginning of significant sediment transport to flows exceeding bankfull discharge. At each transect, eight samples were collected at 0.6-m intervals to represent transport across the channel. A minimum discharge of 1.26 $m^3 s^{-1}$ was required to mobilize measurable amounts of bed load. As is commonly noted in bed load studies, transport was localized over only a small portion of the channel width (e.g., Jackson and Beschta, 1982; Klingeman and Emmett, 1982; Dietrich and Whiting, 1989). Although bed load was concentrated in the zone of high shear stress within approximately 1–2 m of the thalweg, sampling spanned nearly the entire channel width. This avoided bed load bypassing the sampler owing to "topographic steering" (Nelson and Smith, 1989) or deflection by secondary flow (Booker et al., 2001). Therefore, even at high discharge, only trivial amounts of bed load were transported outside the sampled portion of channel. Bed load samples were dried and sieved in the laboratory for particle size analysis.

The Helley–Smith sampler is known to produce biased results in coarse materials (Sterling and Church, 2002). However, there is no consensus regarding the best sampler for obtaining true sediment transport rates in gravel-bed rivers (Ryan and Troendle, 1996; Hassan and Church, 2001). The size of most bed material at our pool centre and tail transects was within the range of high sampler efficiency reported by Emmett (1980); for these two transects we assumed that the Helley–Smith results were reasonable. Sampler efficiency was likely to be somewhat lower at the coarser pool head, imposing some limitation on the analysis of bed load data. To limit error in sampling coarse fractions, we truncated samples at 32 mm. Finally, we assumed that bias in our results was systematic, and therefore comparison among the three transects was reasonable. Similarity of regression relationships for bed load transport rate against discharge among the three transects was tested employing an analysis of covariance approach (Snedecor and Cochran, 1980) and critical probability level of 0.05.

4. Flow dynamics

From observation, flow dynamics and channel morphology were obviously influenced by the primary obstruction adjacent to the deepest part of the pool (Fig. 10.2). It follows that magnitude and distribution of bed shear stress, scour and fill, and sediment entrainment and transport must have also been affected. At all discharges the obstruction deflected flow and elevated shear stress along the base of the slip face of an upstream, left-bank lateral bar, scouring sediment and apparently halting downstream bar migration. In addition, location of a right-bank lateral bar was fixed by deposition in the low-shear stress environment in the lee of the obstruction (Fig. 10.2). Thus, as described by Lisle (1986) for similar obstruction-forced pools, the obstruction anchored the location of both lateral bars, thereby stabilizing channel morphology. These bars further modified streamflow patterns, particularly at moderate and high discharge.

Effects of the obstruction on streamflow patterns can be seen in flow velocity profiles (Fig. 10.3). Profiles selected for Figure 10.3 were representative of flow near the thalweg. These were neither measured at precisely fixed locations nor at the same discharge at all transects. Therefore, these profiles provide a general sense of flow patterns, rather than a rigorous comparison among locations and discharges. At the pool head, obstruction effects

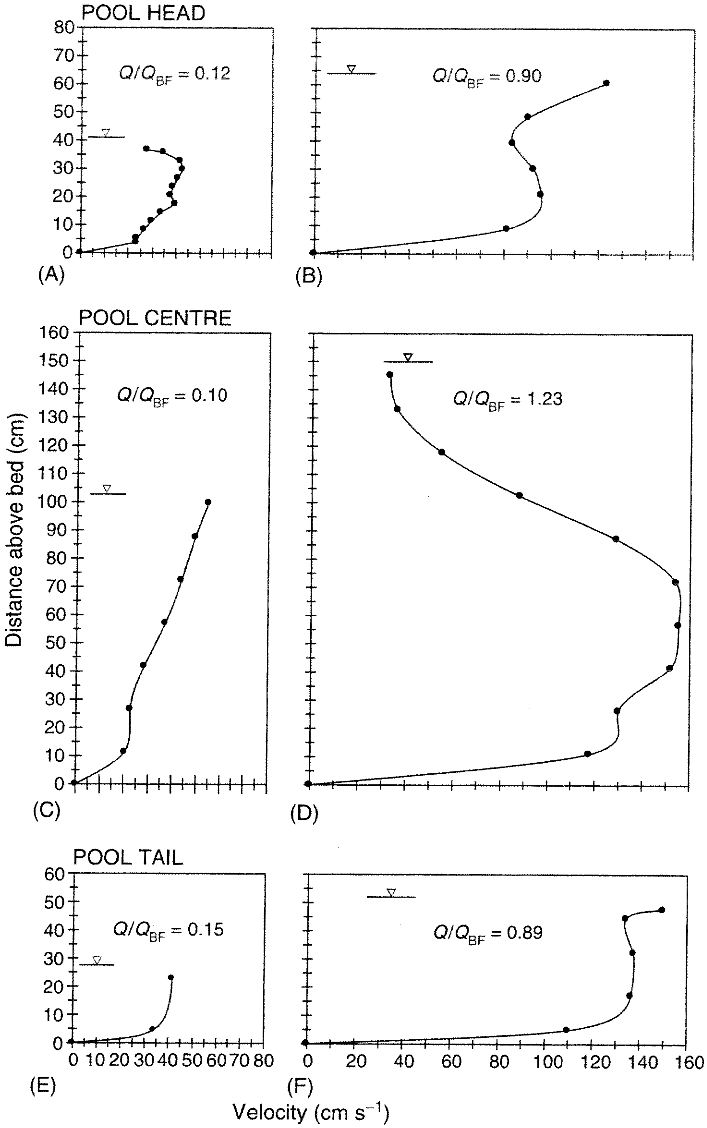

Figure 10.3. Velocity profiles. Q is discharge. Q_{BF} is bankfull discharge. Note scale differences. Triangles indicate water surface elevation.

were minimal at low discharge, therefore velocity profiles were similar to those typical for unobstructed flow, i.e. approximately logarithmic with maximum velocity depressed below the water surface (Fig. 10.3A). As discharge increased above one-half bankfull, backwater effects of the obstruction elevated the water surface on the right side of the channel. This and flow deflection to the left depressed streamwise velocities in the middle portion of the water column, distorting the logarithmic velocity profile (Fig. 10.3B).

Direct effects of the obstruction on streamflow patterns were most pronounced at the pool centre. These effects were evident even at moderate discharge, and included sharp leftward deflection of flow and creation of eddies, vortices, and boils. In addition, a large area of low-velocity, eddying current was created in the downstream lee of the obstruction. At low discharge, vertical velocity distribution was approximately logarithmic, although turbulent structures depressed velocity in the lower-centre of the water column, causing some distortion of the velocity profile (Fig. 10.3C). At high discharge, low shear stress in the lee of the obstruction promoted development of a right-bank lateral bar. This bar reinforced leftward flow deflection by the obstruction, thereby opposing flow deflection by the upstream left bank bar. Flow convergence at the base of the obstruction increased velocity in the lower portion of the water column, while opposing leftward- and rightward-deflected flow created backwater effects, which depressed velocity in the upper water column, thereby strongly distorting the velocity profile (Fig. 10.3D). At the pool tail flow resumed a more streamwise direction, and velocity profiles were generally logarithmic throughout a wide range in discharge (Fig. 10.3E,F).

5. Bed shear stress

Sediment transport and channel morphology were controlled by the magnitude and distribution of boundary shear stress across and along the channel, and the obstruction influenced shear stress distribution through modification of the flow pattern. Figure 10.4 presents variation in shear stress along the three transects at 0.16 Q_{BF}, 0.50 Q_{BF}, and 1.3 Q_{BF}. At low flow at the pool head, the maximum bed shear stress was located slightly to the left of the thalweg and near the toe of the left-bank lateral bar. Maximum shear stress was far less at the pool centre than at the pool head and tail and was located near the thalweg. At the pool tail the channel was wide with approximately uniform bed elevation, grain size distribution, and flow depth. Maximum bed shear stress occurred near the thalweg (Figs 10.2 and 10.4A).

At moderate discharge at the pool head, deflection by the left bank lateral bar forced shear stress maximum toward the right side near the thalweg. At the pool centre the zone of shear stress maximum widened toward the toe of the left-bank lateral bar. Magnitude of shear stress maximum remained markedly smaller than at the pool head or tail. At the pool tail the zone of shear stress maximum became somewhat more focused and shifted toward the toe of the right-bank lateral bar in the lee of the obstruction (Fig. 10.4B).

At flows near or greater than bankfull at the pool head, backwater effects of the obstruction caused location of the shear stress maximum to return toward the left, away from the thalweg and toward the toe of the left-bank lateral bar. Shear stress magnitude was greater than at the pool centre or tail. At the pool centre, shear stress maximum again became focused near the thalweg. At the pool tail flow deflection by the left-bank lateral bar further focused shear stress maxima toward the toe of the right-bank lateral bar (Fig. 10.4C). At all three transects at all measured flows, maximum shear stress location remained within about 1 m of the thalweg.

At all transects, near-bed velocity, averaged over 1 min and over 2.5 m of channel width (the zone of bed load transport), increased linearly with discharge up to flows of at least 1.3 Q_{BF} (Fig. 10.5). At higher discharge, data were more variable; therefore we used

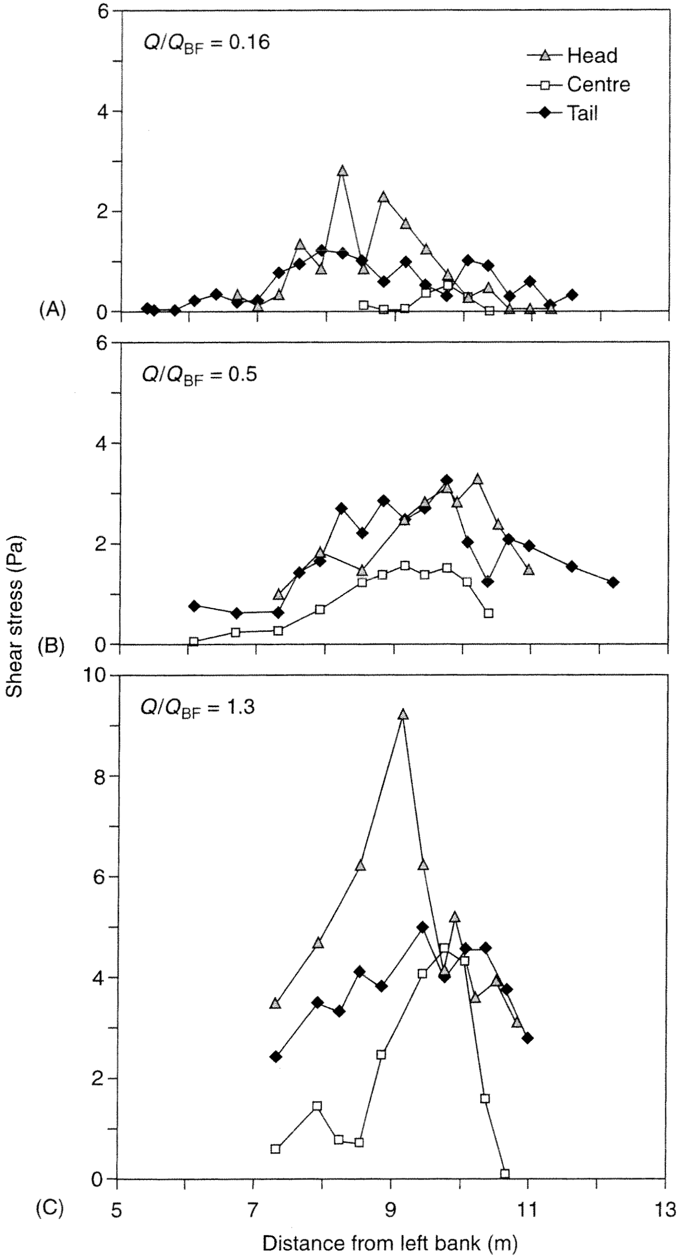

Figure 10.4. Cross-channel variation in bed shear stress at three values of discharge (Q) scaled by bankfull discharge (Q_{BF}).

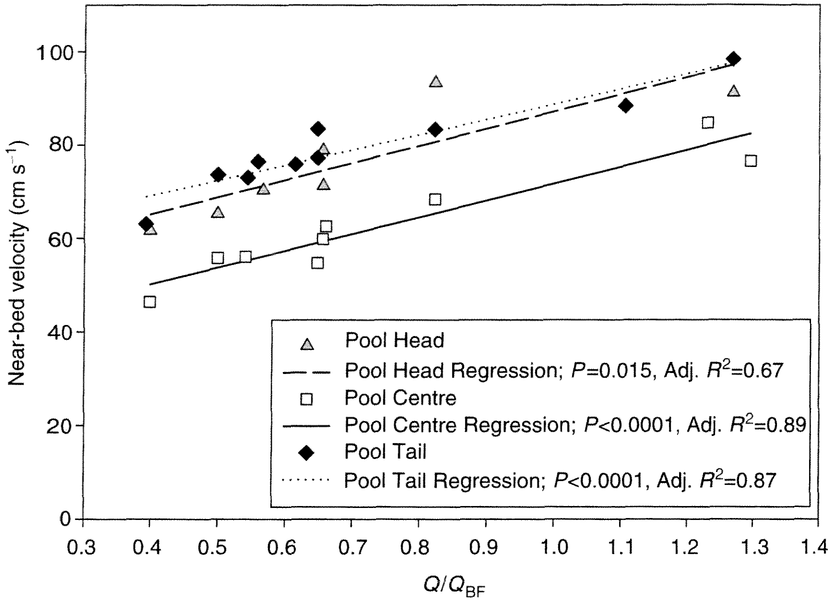

Figure 10.5. Increase in near-bed velocity with dimensionless discharge at the three transects. Straight lines are least squares regression fits to the data.

$Q/Q_{BF} < 1.3$ to define this relationship. Slopes of the regression relationships illustrated in Figure 10.5 were not significantly different among any of the transects, and the intercept for the pool centre relation was significantly less than those for the pool head and tail. Thus, near-bed velocity at the pool centre remained less than that at the pool head and tail, while increasing with discharge at the same rate up to flows at least as large as 1.3 times bankfull (Fig. 10.5).

Similarly the 0.5 power of bed shear stress ($\tau^{0.5}$) increased linearly with dimensionless discharge (Fig. 10.6). Shear stress was transformed to the 0.5 power to stabilize variance and to remove the effect of the increase in shear stress with the square of velocity. Intercepts for the least squares regression relationship illustrated in Fig. 10.6 were statistically different among all transects. Slopes were statistically different for the pool centre and pool tail only. The rate of increase in $\tau^{0.5}$ at the pool tail was the greater. Therefore, bed shear stress at the pool centre remained less than at the pool head and tail, while increasing with dimensionless discharge at the same or lesser rate (Fig. 10.6).

6. Scour and fill

Significant aggradation of both the upstream, left-bank (Fig. 10.7A) and downstream, right-bank (Fig. 10.7C) lateral bars occurred during 24 h surrounding the largest flood peak of the study period. Peak discharge of this event was approximately 7 times bankfull (Fig. 10.8). Aggradation of the upstream bar reduced cross-sectional area at the pool head transect (Fig. 10.7A), and to a much lesser degree and shorter duration, the pool centre transect (Fig. 10.7B). Cross-sectional area of the pool centre, disregarding bank erosion,

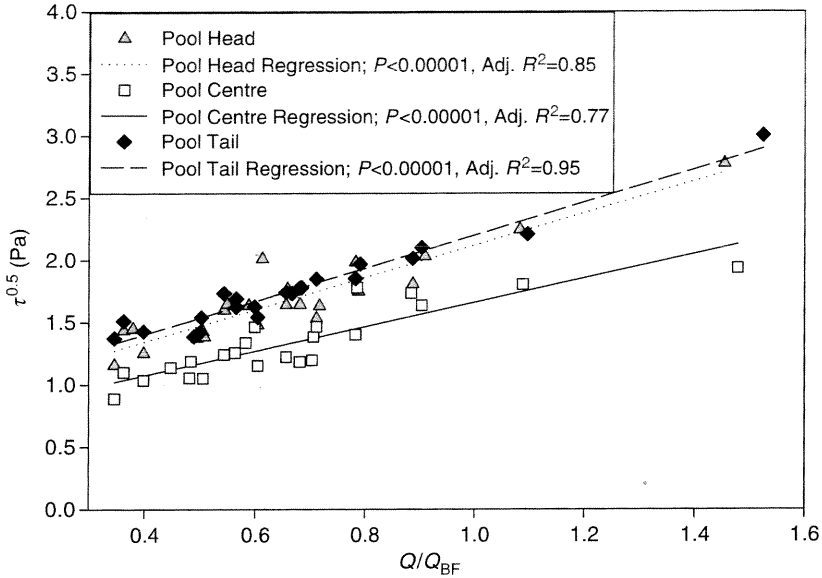

Figure 10.6. Increase in shear stress with dimensionless discharge at the three transects. Straight lines are least squares regression fits to the data.

was remarkably stable throughout a wide range of discharge, including this large flood, which peaked a few hours after the 860217 (17 February 1986) survey (Figs 10.7B, 10.8). Furthermore, subsequent flows eroded much of these bar deposits, returning the bed at the pool centre to nearly the pre-flood profile, disregarding bank erosion (Figs 10.7B, 10.8)

The pool did not store important volumes of sediment relative to the volume transported as bed load. Estimated pool volume was 14.5 m^3, providing a potential storage site for a maximum of 34,000 kg of bed load, assuming a maximum dry density for closely packed silty sand and gravel of 2360 kg m^{-3} (Holtz and Kovacs, 1981). The maximum fill in the pool, in excess of an arbitrary datum, was estimated to be 35% of its volume, deposited primarily on the pool margins during 24 h surrounding the peak discharge. Even this maximum volume of fill did not significantly change pool centre depth (Fig. 10.7B).

During this same period, 84,000 kg of bed load, the equivalent of 250% of the pool volume and 700% of the volume of fill, were transported through the pool. Maximum scour of 17% of the pool volume occurred during the rising limb of the large flood. During this same period, 38,000 kg of bed load were exported, equivalent to 110% of the pool volume and 660% of the volume of scour. These volumes do not include severe bank erosion between days 780 and 785 (Figs 10.7B, 10.8).

Figure 10.7. Cross-sectional soundings. Elevation is relative to an arbitrary datum. The 850514 (14 May 1985) survey provides a common reference in all plots. Post flood bank erosion on the right side of the pool centre is evident in the latest survey.

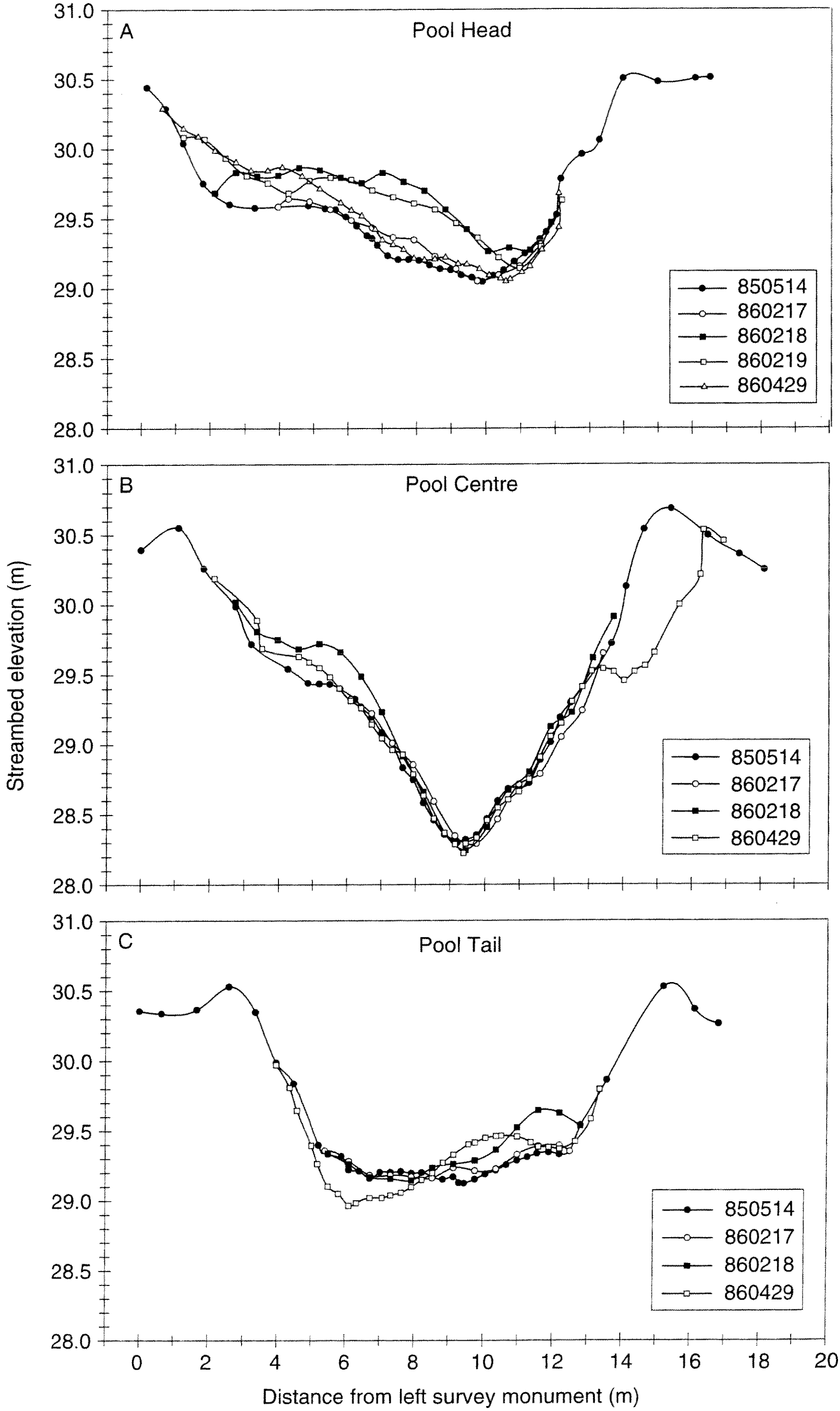
A
Pool Head
B
Pool Centre
C
Pool Tail
850514
860217
860218
860219
860429
Streambed elevation (m)
Distance from left survey monument (m)
31.0
30.5
30.0
29.5
29.0
28.5
28.0
0
2
4
6
8
10
12
14
16
18
20

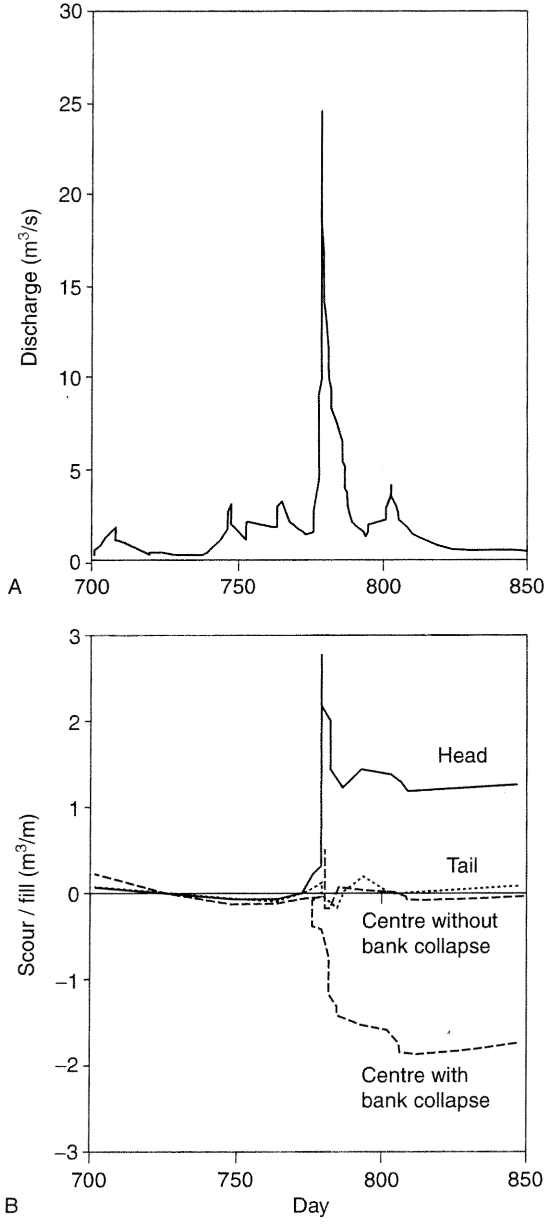

Figure 10.8. Flow hydrograph and scour (−) and fill (+) of the cross-sectional area of the streambed during the primary flood of the study period. Days are expressed numerically, the hydrograph peak occurred on February 17, 1986 (860217, day 778).

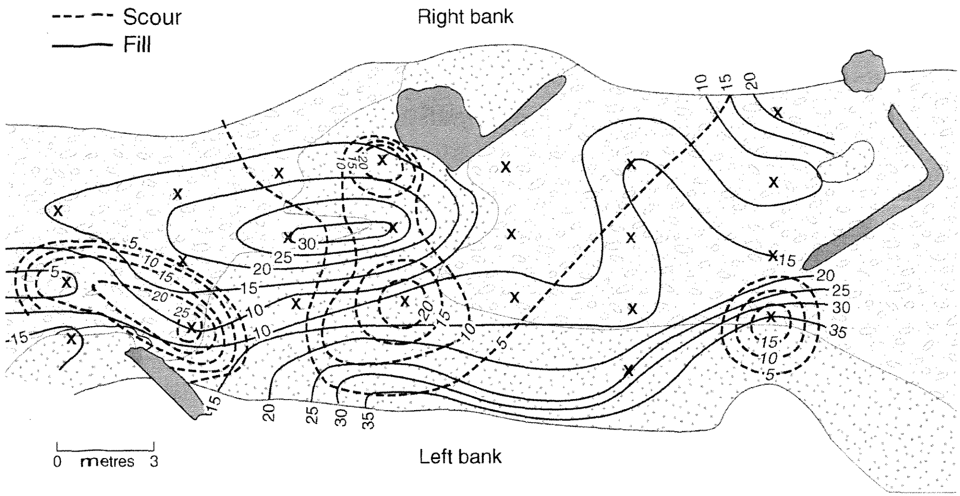

Figure 10.9. Scour and fill, as measured by scour chains, primarily during the major flood of the study period. Scour chain locations are marked with an X. Contour interval is 5 cm.

Scour chain data indicated zero net average change in the bed surface elevation at the pool centre (Fig. 10.9). However, soundings, unlike scour chain data, included the banks and indicated major lateral erosion of the right bank, resulting from flow deflection by the obstruction during the receding limb of the largest flood (Fig. 10.8). Disregarding bank erosion, both scour chains and soundings indicated very minor net change to the pool centre bed profile during the study period (Figs 10.7–10.9).

7. Sediment entrainment

To examine the relation between fractional sediment transport and shear stress for each bed load size fraction, the size-specific scaled fractional transport rate was plotted against particle size over a range of shear stress magnitude (Fig. 10.10A–C). The fractional transport rate was scaled using the subsurface material grain size distribution averaged over all three transects and truncated at 32 mm, because of limitations of the Helley–Smith sampler and uncertain sampling of material larger than 32 mm diameter. All curves show a break in slope where transport rate begins to decline with increasing grain size, i.e. a shift from full to partial mobility (Fig. 10.10A–C). Dark lines in Figure 10.10 connect break points in fractional mobility, which represent the largest fully mobile grain size for each value of shear stress. The increase in this grain size with shear stress implies selective transport.

Following the Wilcock and McArdell (1993) method, the critical shear stress needed to initiate transport for a given fraction was taken from the Parker et al. (1982) reference transport relations, covering most of the range of transported material (Fig. 10.10D). The reference shear stress is that needed to entrain an individual size fraction and produce

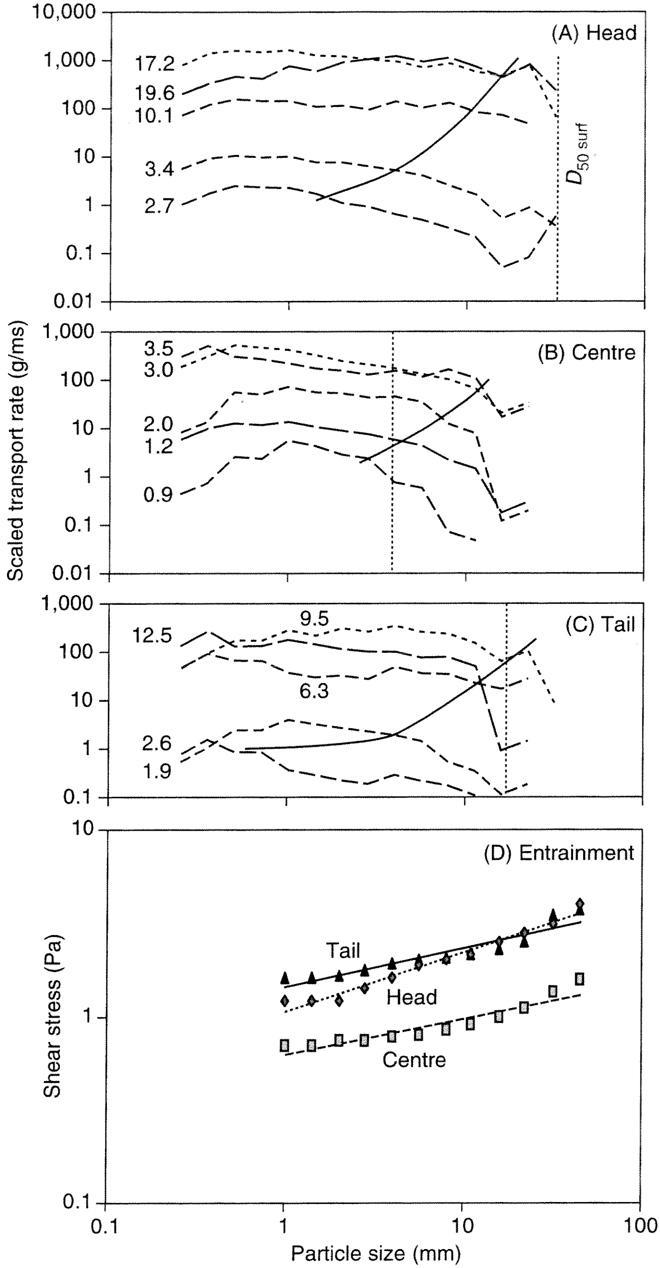

Figure 10.10. Scaled fractional sediment transport rate versus particle size for selected flows, shown as the associated bed shear stress (Pa): (A) pool head; (B) pool centre; (C) pool tail. The median size of the bed surface is plotted for comparison. (D): the relation between particle size and bed shear stress needed to initiate movement of individual particles.

a small reference transport rate. The fitted functional relations are as follows:

$$\tau_{ri} = 1.05 \pm 0.09 D_i^{0.32 \pm 0.016} \quad \text{for the pool head} \tag{4}$$

$$\tau_{ri} = 0.62 \pm 0.08 D_i^{0.19 \pm 0.022} \quad \text{for the pool centre} \tag{5}$$

$$\tau_{ri} = 1.43 \pm 0.17 D_i^{0.21 \pm 0.024} \quad \text{for the pool tail} \tag{6}$$

where D_i is the particle size in mm, and τ_{ri} is the reference shear stress in Pascal. These incipient motion analyses suggest that mean bed shear stress entrainment thresholds for the range of grain sizes measured were lower (entrainment at lower shear stress) at the pool centre than at the pool head or tail (Fig. 10.10D) (Hassan and Woodsmith, 2004).

We further examined bed load entrainment by analyzing the relationship between the intermediate diameter of the largest clast in each bed load sample and the dimensionless shear stress (Fig. 10.11). Due to sampling bias of the Helley–Smith sampler (discussed in

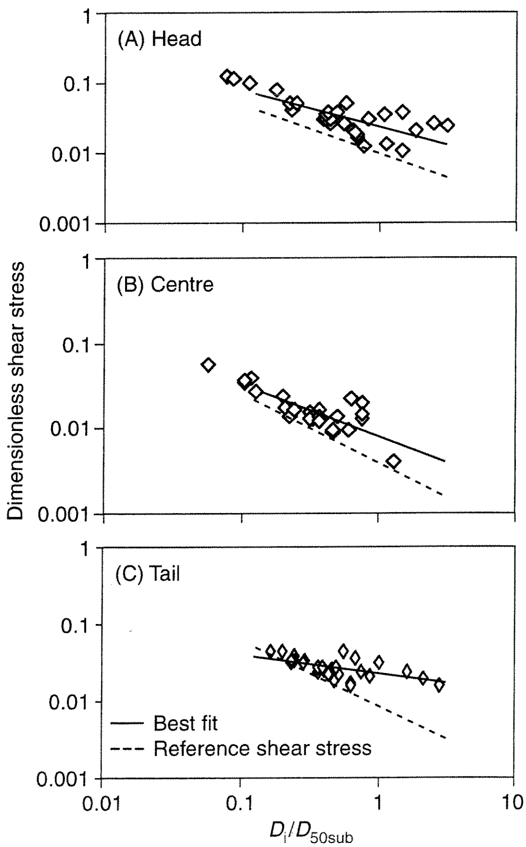

Figure 10.11. Dimensionless shear stress as a function of relative grain size (scaled to the median diameter of the subsurface material). In this plot we used the largest clast found in the sampler. The best-fit line and the reference shear stress (Eqs. 4–6) are shown.

Sterling and Church, 2002; Hassan and Woodsmith, 2004), these analyses should be viewed as an approximation of entrainment conditions. The relations for the data presented in Figure 10.11 are as follows,

$$\tau_{ri^*} = 0.023 \pm 0.004(D_{i\text{-max}}/D_{50sub})^{-0.51\pm0.07} \quad \text{for the pool head} \quad (7)$$

$$\tau_{ri^*} = 0.008 \pm 0.003(D_{i\text{-max}}/D_{50sub})^{-0.60\pm0.12} \quad \text{for the pool centre} \quad (8)$$

$$\tau_{ri^*} = 0.022 \pm 0.005(D_{i\text{-max}}/D_{50sub})^{-0.27\pm0.10} \quad \text{for the pool tail} \quad (9)$$

where the dimensionless shear stress (τ_{ri^*}) = $\tau_b[(\rho_s\text{-}\rho)gD_i]^{-1}$, ρ_s is the sediment density, g is gravitational acceleration, $D_{i\text{-max}}$ is the largest particle in the bed load sample, and D_{50sub} is the median size of the subsurface bed material. A slope of -1.0 would imply equal mobility (Parker and Klingeman, 1982), therefore a strong relative size effect on entrainment of individual particles is suggested, implying that selective entrainment occurs along the three transects.

For comparison, we plotted Eqs. (4–6), the reference transport relations, using the same units as in the dimensionless Eqs. (7–9). In all cases the reference transport line plots near the lower limit of the data (Fig. 10.11). The reference transport line represents the lower limit for entrainment, below which no sediment transport is expected. Similar results were reported in Church and Hassan (2002) for data from Harris Creek, British Columbia, Canada.

8. Bed load transport rates

High bed load transport rates at the pool tail ($G_{\text{-tail}}$) were clearly associated with high discharge (Table 10.1). Nevertheless, highly variable $G_{\text{-tail}}/G_{\text{-head}}$ ratios for consecutive samples, collected within several minutes of one another together with minor change in pool cross-sectional area suggested that dynamic upstream sediment supply was a primary control on bed load transport. Regular patterns of pool filling ($G_{\text{-tail}}/G_{\text{-head}} < 1$) at low discharge and pool scour ($G_{\text{-tail}}/G_{\text{-head}} > 1$) at discharge above bankfull were not apparent in our data (Table 10.1). For example, several days after the 860217 flood at $Q/Q_{BF} = 0.35$, $G_{\text{-tail}}$ exceeded $G_{\text{-head}}$ by a factor of nearly 8; however, only 5 days later at $Q/Q_{BF} = 0.54$, $G_{\text{-head}}$ exceeded $G_{\text{-tail}}$ by a factor of 2.5 (Table 10.1). For $2 < Q/Q_{BF} < 3$, $G_{\text{-tail}}/G_{\text{-head}}$ varied from 0.4 to 17.4. These examples are extreme cases, nevertheless there was no consistent pattern of pool scour and fill, as measured by $G_{\text{-tail}}/G_{\text{-head}}$, in response to discharge magnitude. Similarly, there was no clear correlation between $G_{\text{-tail}}/G_{\text{-head}}$ and hydrograph limb. The four largest values of $G_{\text{-tail}}$ occurred within the first week following the 860217 flood peak (Table 10.1).

Bed load transport rate increased with discharge at all transects. Sensitivity (slope) of the rating relation changed at a critical discharge of about Q_{BF} (Fig. 10.12). Below Q_{BF}, sediment transport rate increased rapidly as discharge increased, but increased more slowly at flows above Q_{BF}. Piecewise regression, was employed to compare the rating equations among transects using Q_{BF} as a critical value (Fig. 10.12) (also see Ryan et al., 2002). Increase in bed load transport rate with discharge was not significantly different in the pool centre from that at the pool head or tail ($P = 0.05$). However, close proximity of

Table 10.1. Bed load Flux. Q is water discharge. Q_{BF} is bankfull discharge. G is bed load transport rate (kg h^{-1}). Rows are arranged in order of increasing discharge. Bed load export through the pool is indicated by $G_{-tail}/G_{-head} > 1.0$. Dates are expressed numerically as year, month, and day.

Q ($m^3 s^{-1}$)	Q/Q_{BF}	G_{-tail}/G_{-head}	G_{-tail} (kg h^{-1})	Hydrograph limb	Date
1.26	0.35	7.9	7.7	Falling	860304
1.32	0.36	0.9	4.8	Falling	860120
1.45	0.40	1.4	7.5	Falling	860320
1.78	0.49	0.9	5.9	Rising	860116
1.82	0.50	1.1	7.1	Rising	860122
1.83	0.50	1.4	21	Falling	860318
1.98	0.54	0.4	27	Rising	860309
2.06	0.57	0.5	9.1	Rising	860214
2.06	0.57	0.9	310	Falling	860308
2.18	0.60	0.9	9.2	Falling	860206
2.21	0.61	1.6	58	Falling	860311
2.39	0.66	1.4	46	Falling	860316
2.43	0.67	3.0	100	Rising	860202
2.48	0.68	2.1	69	Falling	860311
2.49	0.68	5.1	1300	Falling	860307
2.60	0.71	5.2	32	Falling	860205
2.85	0.78	3.1	30	Falling	860204
2.88	0.79	47.7	3200	Falling	860315
3.23	0.89	3.6	170	Peak	860203
3.29	0.90	0.5	1300	Falling	860226
3.99	1.10	0.6	1100	Falling	860313
5.56	1.53	4.5	3200	Rising	860216
5.86	1.61	1.0	4100	Falling	860224
7.41	2.03	0.4	890	Falling	860216
7.78	2.14	17.4	41,000	Rising	860221
10.6	2.93	0.6	1900	Rising	860217
12.1	3.32	0.5	8900	Rising	860219
12.9	3.55	2.2	56,000	Rising	860219

the three transects may have masked spatial variations, making this observation difficult to interpret.

9. Discussion

We observed that the primary obstruction in the study reach influenced flow dynamics and channel morphology through flow deflection and convergence and creation of turbulent structures including eddies, vortices, and boils forced by flow-obstruction interaction. To quantify obstruction effects we compared velocity distribution, bed shear stress, streambed scour and fill, and bed load transport rate and grain-size distribution among nonobstruction-related pools. The role of smaller-scale turbulence in nonobstruction related sediment entrainment is well established (Kalinske, 1947; Sutherland, 1967; Baker and Ritter, 1975; Cheetham, 1979; Carling, 1983; Whiting and Dietrich, 1990; Nelson et al., 1995). We were not able to quantify obstruction related turbulence with direct measurements. Such measurements remain problematic in gravel-bed streams, owing to the mobile boundary and risk of damage to instruments (Whiting and Dietrich, 1990; Bunte, 1996).

10. Conclusions

Our results, observations of turbulent structures, and analogy to well known processes of scour at bridge abutments and piers support a conceptual model explaining maintenance of obstruction-forced pools at naturally occurring flow obstructions in gravel-bed streams. Analogous hydraulic conditions of fluvial scour around bridge abutments and piers are common, where bed material is mobilized by a combination of time-averaged bed shear stress and turbulent agitation in the scour hole (Melville, 1975; Breusers et al., 1977). In this case study, as in the case of bridge abutments and piers, turbulent effects generated by interaction of streamflow with the obstruction contribute an additional component of total force acting to entrain and transport sediment. Pool maintenance results from a combination of mean bed shear stress and these large-scale turbulent drags and lift forces. At discharge above the transport threshold for the upstream bed, bed load moves through the pool centre in response to sediment delivery from upstream, causing multiple pulses of bed load through the pool during a single storm hydrograph. Following the discharge peak, bed load flux drops when upstream shear stress decreases to the point that bed load is no longer delivered to the pool (Lisle, 1986; Smith, 1990; Buffington et al., 2002).

This model provides an alternative to the velocity reversal hypothesis, which describes pool maintenance in free-formed alluvial pools, rather than obstruction-forced pools. Our results do not refute the velocity reversal hypothesis, rather we argue simply that flow hydraulics in obstruction-forced pools can differ from those in free-formed pools. Clearly, competence in any pool must at times be sufficient to transport material delivered from upstream in order to maintain pool volume. However, our data indicate that maintenance of the study pool, formed by scour at a large in-channel obstruction, is attributable to processes other than shifting of the location of maximum near-bed velocity or bed shear stress to the pool centre at high discharge. We conclude that obstruction-forced pools do not necessarily undergo alternate scour and fill patterns during high and low flow sequences as suggested by the velocity reversal hypothesis. Rather, pool volume can remain remarkably stable throughout a wide range in discharge.

We emphasize the unique nature of obstruction-forced pools where large-scale turbulent structures generated by interactions of flow with the obstruction appear to generate entrainment and tractive forces that alter the shear stress-sediment transport relationship relative to upstream and downstream riffles. Although turbulence was not directly measured, it remains the likely factor to make up for relatively low values of mean shear stress in pools, thereby maintaining necessary competence for pool maintenance. This combination of mean bed shear stress and instantaneous turbulent force creates and maintains the pool at a site where scour may not have occurred in the absence of an obstruction.

Our results suggest that scour forced by large, in-channel obstructions can be a dominant mechanism, perhaps as important as mean hydraulic variables and caliber and volume of sediment supply, explaining local channel morphology and local bed load dynamics. However, pool scour varies with size and shape of obstructions and with drainage basin and channel characteristics (Buffington et al., 2002). Extrapolation of results of this study to other obstruction-pool geometries is untested.

Results of this study are of interest not only to fluvial geomorphologists, but also to engineers and land managers involved with aquatic habitat restoration through manipulation of channel morphology. These results provide insight into the mechanisms responsible for scour and maintenance of pools associated with either naturally occurring or artificially placed obstructions. Local hydraulics, channel morphology, and sediment transport can mutually adjust to large, in-channel obstructions in such a way that the associated pool morphology is maintained through a wide range in discharge. This dynamic stability may provide critical habitat with a wide diversity of water depth and velocity for aquatic organisms, including refuge habitat during high-flow conditions.

Acknowledgements

This research was supported by USDI, Redwood National Park; USDA, Forest Service, Pacific Northwest Research Station; and the Natural Sciences and Engineering Research Council of Canada through Research grant 249673 to M. Hassan. Jason Rempel performed part of the sediment transport analyses, and Eric Leinberger prepared the figures. Tim Max, USDA Forest Service, Pacific Northwest Research Station provided statistical advice. John Buffington, Tom Lisle, and Dave Montgomery provided insightful reviews. Their comments and suggestions greatly improved the manuscript.

References

Adams, S.B., Frissell, C.A., Rieman, B.E., 2000. Movements of nonnative brook trout in relation to stream channel slope. Trans. Am. Fish. Soc. 129, 623–638.

Andrews, E.D., 1979. Scour and fill in a stream channel, East Fork River, western Wyoming. U.S. Geol. Surv. Prof. Pap. 1117, 49.

Ashworth, P.J., 1987. Bedload transport and channel change in gravel-bed rivers. Ph.D. Thesis, University of Stirling, Scotland, 352 pp.

Baker, V.R., Ritter, D.F., 1975. Competence of rivers to transport coarse bedload material. Geological Survey, Professional Paper 86, 975–978.

Beschta, R.L., 1981. Increased Bag Size Improves Helley–Smith Bedload Sampler for Use in Streams with High Sand and Organic Matter Transport, Erosion and Sediment Transport Measurement, Vol. 133. IAHS Publisher, Vienna, pp. 17–25.

Beschta, R.L., 1983. Effects of Large Organic Debris on Channel Morphology, D.B. Simons Symposium on Erosion and Sedimentation. Simons, Li, & Association, Fort Collins, Colorado, pp. 8.63–8.78.

Booker, D.J., Sear, D.A., Payne, A.J., 2001. Modeling three-dimensional flow structures and patterns of boundary shear stress in a natural pool-riffle sequence. Earth Surf. Processes Land. 26, 553–576.

Breusers, H., Nicollet, G., Shen, H., 1977. Local scour around cylindrical piers. J. Hydraul. Res. 15, 211–252.
Buffington, J.M., Montgomery, D.R., 1999a. Effects of hydraulic roughness on surface textures of gravel-bed rivers. Water Resour. Res. 35, 3507–3522.
Buffington, J.M., Montgomery, D.R., 1999b. Effects of sediment supply on surface textures of gravel-bed rivers. Water Resour. Res. 35, 3523–3530.
Buffington, J.M., Lisle, T.E., Woodsmith, R.D., Hilton, S., 2002. Controls on the size and occurrence of pools in coarse-grained forest rivers. River Res. Appl. 18, 507–531.
Bunte, K., 1996. Analyses of the temporal variation of coarse bedload transport and its grain size distribution (Squaw Creek, Montana, USA). RM-GTR-288, USDA, Forest Service, Rocky Mountain Forest and Range Experiment Station, Fort Collins, CO.
Cao, Z., Carling, P., Oakey, R., 2003. Flow reversal over a natural pool-riffle sequence: a computational study. Earth Surf. Processes Land. 28, 689–705.
Carling, P.A., 1983. Threshold of coarse sediment transport in broad and narrow natural streams. Earth Surf. Processes Land. 8, 1–18.
Carling, P.A., Wood, N., 1994. Simulation of flow over pool-riffle topography: a consideration of the velocity reversal hypothesis. Earth Surf. Processes Land. 19, 319–332.
Carstens, M.R., 1966. Similarity laws for localized scour. J. Hydraul. Div., Am. Soc. Civ. Eng. 92, 13–16.
Chabert, J., Engeldinger, P., 1956. Etude des affouillements autour des piles des ponts. Laboratoire National d'Hydraulique, Chatou, France.
Cheetham, G.H., 1979. Flow competence in relation to stream channel form and braiding. Geol. Soc. Am. Bull. 90, 877–886.
Church, M., Jones, D., 1982. Channel Bars in Gravel-bed Rivers. In: Hey, R.D., Bathurst, J.C., Thorne, C.R. (Eds), Gravel-bed Rivers. Wiley, New York, pp. 291–338.
Church, M., Hassan, M.A., 2002. Mobility of bed material in Harris Creek. Water Resour. Res. 38, 101029/2001WR000753.
Clifford, N.J., Richards, K.S., 1992. The reversal hypothesis and the maintenance of riffle-pool sequences: a review and field appraisal. In: Carling, P.A., Petts, G.E. (Eds), Lowland Floodplain Rivers: Geomorphological Perspectives. Wiley, Chichester, UK, pp. 43–70.
Dietrich, W.E., Whiting, P., 1989. Boundary shear stress and sediment transport in river meanders of sand and gravel. In: Ikeda, S., Parker, G. (Eds), River Meandering. American Geophysical Union, Washington, pp. 1–50.
Dietrich, W.E., Smith, J.D., Dunne, T., 1979. Flow and sediment transport in a sand bedded meander. J. Geol. 87, 305–315.
Dietrich, W.E., Kirchner, J.W., Ikeda, H., Iseya, F., 1989. Sediment supply and the development of the coarse surface layer in gravel-bedded rivers. Nature 340, 215–217.
Emmett, W.W., 1980. A field calibration of the sediment trapping characteristics of the Helley–Smith bedload sampler, U.S. Geological Survey, Professional Paper 1139. Washington, DC, p. 44.
Emmett, W.W., Leopold, L.B., Myrick, R.M, 1983. Some characteristics of fluvial processes in rivers. Proc. Second International Symposium on River Sedimentation. Water Resources and Electric Power Press, Nanjing, China, pp. 730–754.
Freshwater Ecosystems 5, 143–166.
Gomez, B., Naff, R.L., Hubbell, D.W., 1989. Temporal variation in bedload transport rates associated with the migration of bedforms. Earth Surf. Processes Land. 14, 135–156.
Gurnell, A.M., Gregory, K.J., Petts, G.E., 1995. The role of coarse woody debris in forest aquatic habitats: implications for management. Aquat. Conserv. Mar. Fresh. Ecosyst. 5, 143–166.
Hassan, M.A., Church, M., 2001. Rating bed load transport in Harris Creek: seasonal and spatial variation over a cobble-gravel bed. Water Resour. Res. 37, 813–825.
Hassan, M.A., Woodsmith, R.D., 2004. Bed load transport in an obstruction-formed pool in a forest, gravel-bed stream. Geomorphology 58, 203–221.
Helley, E.J., Smith, W., 1971. Development and Calibration of a Pressure Difference Bedload Sampler. Open File Report 73-108, U.S. Geological Survey, Washington, D.C.
Hey, R.D., 1979. Flow resistance in gravel-bed rivers. J. Hydraul. Div., Am. Soc. Civ. Eng. 107, 365–379.
Hogan, D.L., Bird, S.A., Hassan, M.A., 1998. Spatial and temporal evolution of small coastal gravel-bed streams: the influence of forest management on channel morphology and fish habitat. In: Klingeman, P.C., Beschta, R.L., Komar, P.D., Bradley, J.B. (Eds), Gravel-Bed Rivers in the Environment. Water Resources Publications, LLC, Highland Ranch, Colorado, pp. 365–392.

Holtz, R.D., Kovacs, W.D., 1981. An Introduction to Geotechnical Engineering. Prentice-Hall, Englewood Cliffs, NJ, p. 733.

Jackson, W.L., Beschta, R.L., 1982. A model of two-phase bedload transport in an Oregon Coast Range stream. Earth Surf. Processes Land. 7, 517–527.

Kalinske, A.A., 1947. Movement of sediment as bed in rivers. Trans. Am. Geophys. Union 28, 615–620.

Keller, E.A., 1971. Areal sorting of bed load material: the hypothesis of velocity reversal. Geol. Soc. Amer. Bull. 82, 753–756.

Keller, E.A., Florsheim, J.L., 1993. Velocity-reversal hypothesis: a model approach. Earth Surf. Processes Land. 18, 733–740.

Keller, E.A., Swanson, F.J., 1979. Effects of large organic material on channel form and fluvial processes. Earth Surf. Processes Land. 4, 361–380.

Klingeman, P.C., Emmett, W.W., 1982. Gravel bedload transport processes. In: Hey, R.D., Bathurst, J.C., Thorne, C.R. (Eds), Gravel-bed Rivers. Wiley, New York, pp. 141–179.

Kuhnle, R.A., Southard, J.B., 1988. Bed load transport fluctuations in a gravel bed laboratory channel. Water Resour. Res. 24, 247–260.

Leopold, L.B., Wolman, M.G., 1960. River Meanders. Geol. Soc. Am. Bull. 71, 769–794.

Leopold, L.B., Wolman, M.G., Miller, J.P., 1964. Fluvial Processes in Geomorphology. W.H. Freeman, San Francisco, CA, p. 522.

Lisle, T.E., 1979. A sorting mechanism for a riffle-pool sequence. Geol. Soc. Am. Bull. 90, 1142–1157.

Lisle, T.E., 1982. Effects of aggradation and degradation on riffle-pool morphology in natural gravel channels, Northwestern California. Water Resour. Res. 18, 1643–1651.

Lisle, T.E., 1986. Stabilization of a gravel channel by large streamside obstructions and bedrock bends, Jacoby Creek, Northwestern California. Geol. Soc. Am. Bull. 97, 999–1011.

Melville, B.W., 1975. Local scour at bridge sites. Ph.D. Thesis, University of Auckland, N.Z.

Melville, B.W., 1984. Live-bed scour at bridge piers. J. Hydraul. Eng. 110, 1234–1247.

Melville, B., 1997. Pier and abutment scour: integrated approach. J. Hydraul. Eng. 123, 125–136.

Melville, B.W., Sutherland, A.J., 1988. Design method for local scour at bridge piers. J. Hydraul. Eng. 114, 1210–1226.

Meyer-Peter, E., Muller, R., 1948. Formulas for Bed-load Transport, 3rd Annual Conference. International Association of Hydraulic Research, Stockholm, pp. 39–64.

Middleton, G.V., Southard, J.B., 1984. Mechanics of sediment movement, short course NBno. 3. Soc. Econ. Paleontologists and Mineralogists, Tulsa, OK, p. 401.

Montgomery, D.R., Buffington, J.M., Smith, R.D., Schmidt, K.M., Pess, G., 1995. Pool spacing in forest channels. Water Resources Research, 31, 1097–1105.

Montgomery, D.R., Buffington, J.M., 1997. Channel-reach morphology in mountain drainage basins. Geol. Soc. Am. Bull. 109, 596–611.

Nelson, J.M., Smith, J.D., 1989. Evolution and stability of erodible channel beds. In: Ikeda, S., Parker, G. (Eds), River Meandering. American Geophysical Union, Washington, pp. 321–377.

Nelson, J.M., Shreve, R.L., McLean, S.R., Drake, T.G., 1995. Role of near-bed turbulence structure in bed load transport and bed load mechanics. Water Resour. Res. 31, 2071–2086.

Paola, C., Mohrig, D., 1996. Paleohydraulics revisited: paleoslope estimation in coarse-grained braided rivers. Basin Res. 8, 243–254.

Parker, G., Klingeman, P.C., 1982. On why gravel bed streams are paved. Water Resour. Res. 18, 1409–1423.

Parker, G., Peterson, A.W., 1980. Bar resistance of gravel-bed streams. J. Hydraul. Div., Am. Soc. Civ. Eng. 106, 1559–1575.

Parker, G., Klingeman, P.C., McLean, D.L., 1982. Bed load and size distribution in paved gravel-bed streams. J. Hydraul. Div. ASCE 108, 544–571.

Piegay, H., Gurnell, A.M., 1997. Large woody debris and river geomorphological pattern: examples from S.E. France and S. England. Geomorphology 19, 99–116.

Pitlick, J., 1988. Variability of bed load measurement. Water Resour. Res. 24, 173–177.

Prestegaard, K.L., 1983. Bar resistance in gravel-bed streams at bankfull stage. Water Resour. Res. 19, 472–476.

Ranch, Colorado, pp.365–392.

Richards, K.S., 1976. The morphology of riffle-pool sequences. Earth Surf. Processes Land. 1, 71–88.

Robert, A., 1997. Characteristics of velocity profiles along riffle-pool sequences and estimates of bed shear stress. Geomorphology 19, 89–98.

Ryan, S.E., Troendle, C.A., 1996. Bed Load Transport Patterns in Coarse-Grained Channels under Varying Conditions of Flows, Sedimentation Technologies for Management of Natural Resources in the 21st Century; Proceedings of Sixth Federal Interagency Sedimentation Conference, Las Vegas, NV, pp. VI-22–VI-27.

Ryan, S.E., Porth, L.S., Troendle, C.A., 2002. Defining phases of bedload transport using piecewise regression. Earth Surf. Processes Land. 27, 971–990.

Sear, D.A., 1996. Sediment transport processes in pool-riffle sequences. Earth Surf. Processes Land. 21, 241–262.

Smith, R.D., 1990. Streamflow and bedload transport in an obstruction-affected, gravel-bed stream. Ph.D. Thesis, Oregon State University, Corvallis, Oregon, p. 181.

Smith, R.D., Sidle, R.C., Porter, P.E. and Noel, J.R., 1993. Effects of experimental removal of woody debris on the channel morphology of a forest, gravel-bed stream. Journal of Hydrology 152, 153–178.

Snedecor, G.W., Cochran, W.G., 1980. Statistical Methods. Iowa St. Univ. Press, Ames, Iowa, p. 507.

Sterling, S., Church, M., 2002. Sediment trapping characteristics of a pit trap and a Helley–Smith sampler in a cobble-gravel bed river. Water Resour. Res. 38, 101029/2000WR000052.

Sutherland, A.J., 1967. Proposed mechanism for sediment entrainment by turbulent flows. Journal of Geophysical Research 72, 6183–6194.

Thompson, D.M., Wohl, E.E., Jarrett, R.D., 1996. A revised velocity-reversal and sediment-sorting model for a high-gradient, pool-riffle stream. Phys. Geogr. 17 (2), 142–156.

Thompson, D.M., Wohl, E.E., Jarrett, R.D., 1999. Velocity reversals and sediment sorting in pools and riffles controlled by channel constrictions. Geomorphology 27, 229–241.

Tison, L.J., 1961. Local scour in rivers. J. Geoph. Res. 66, 4227–4232.

Whiting, P.J., Dietrich, W.E., 1990. Boundary shear stress and roughness over mobile alluvial beds. J. Hydraul. Eng. 116, 1495–1511.

Wilcock, P.R., 1992. Flow competence: a criticism of a classic concept. Earth Surf. Processes Land. 17, 289–298.

Wilcock, P.R., McArdell, B.W., 1993. Surface-based fractional transport rates: mobilization thresholds and partial transport of a sand-gravel sediment. Water Resources Research 29, 1297–1312.

Wilkinson, S.N., Keller, R.J., Rutherfurd, I.D., 2004. Phase-shifts in shear stress as an explanation for the maintenance of pool-riffle sequences. Earth Surf. Processes Land. 29, 737–753.

Woodsmith, R.D., Buffington, J.M., 1996. Multivariate geomorphic analysis of forest streams: implications for assessment of land use impacts on channel condition. Earth Surf. Processes Land. 21, 377–393.

Woodsmith, R.D., Swanson, F.J., 1997. The influence of large woody debris on forest stream geomorphology. In: Wang, S.S.Y., Langedoen, E.J., Shields, F.D.J. (Eds), Management of Landscapes Disturbed by Channel Incision. University of Mississippi, Oxford, MS, pp. 133–138.